Cytosine-phosphodiester-Guanine Oligodeoxynucleotide (CpG ODN)-Capped Hollow Mesoporous Silica Particles for Enzyme-Triggered Drug Delivery

Yufang Zhu[a]*, Wenjun Meng[b], Nobutaka Hanagata[b,c]

a) *School of Materials Science and Engineering, University of Shanghai for Science and Technology, 516 Jungong Road, Shanghai, 200093, P. R. China.*

b) *Graduate School of Life Science, Hokkaido University, N10W8, Kita-ku, Sapporo, 060-0812, Japan.*

c) *Interdisciplinary Laboratory for Nanoscale Science and Technology, National Institute for Materials Science, 1-2-1 Sengen, Tsukuba, Ibaraki, 305-0047, Japan.*

Corresponding author:

Dr. Yufang Zhu:

Tel: +86-21-55271663

Email: zjf2412@163.com

Abstract: We designed, for the first time, an enzyme-triggered drug delivery system that is based on cytosine-phosphodiester-guanine oligodeoxynucleotide (CpG ODN)-capped hollow mesoporous silica (HMS) particles as carriers. Fluorescein dye was used as a model drug, and the fluorescein loading, amino-grafting and CpG ODN capping were evaluated by UV/Vis analysis, zeta potential and N_2 adsorption-desorption measurements and gel electrophoresis. The fluorescein loading capacity and CpG ODN capping amount were 37.7 and 39.6 μg/mg, respectively at the weight ratio of 10 Dye/HMS-NH_2/CpG ODN. Importantly, fluorescein release can be triggered by the addition of deoxyribonuclease I (DNase I) for CpG ODN degradation, and the release rate can also be controlled by changing the DNase I concentration. Therefore, it might be a promising controlled drug delivery system for application in the field of biomedicine and cancer therapy.

Keywords: Hollow mesoporous silica, Controlled release, CpG ODN, Drug delivery

Introduction

Mesoporous silica nanoparticles (MSNs) have high surface area and pore volume, tunable pore size, well-defined surface properties for modification, and biocompatibility, which provides a stable carrier for drug loading and release.[1-3] In recent years, as an alternative to polymeric materials, MSNs have been widely studied as inorganic carriers for drug delivery.[4-11]

It has been accepted that stimuli-responsive drug delivery could significantly reduce the serious side effects associated with many toxic drugs and enhance the therapeutic efficacy. Therefore, many efforts have been made to design and construct the gated MSNs carriers for stimuli-responsive drug delivery.[12-21] The first gated MSNs carriers were developed by M. Fujiwara and co-workers via the reversible photodimerization of coumarin grafted to the mesopore openings of MCM-41 that was sensitive to light.[12] Since then, various components, such as CdS, Fe_3O_4 and Au nanoparticles,[13-15] collagen,[16] oligonucleotide,[17-18] antibody,[19] supermolecules,[20] and polyelectrolyte,[21] have been used to construct the gated MSNs carriers for controlled drug release, and these components respond to a range of stimuli including redox, pH or temperature, competitive binding, and so on. For example, Lai et al. developed a gated MSNs system, where the mesopores loaded with guest molecules were capped by CdS nanoparticles via a chemically cleavable disulfide linkage to the MSN surface, and the release was triggered by the addition of dithiothreitol (DTT) to cleave the disulfide linker.[15] We proposed a concept to design a pH-responsive controlled drug release system by using the pH-responsive polyelectrolyte multilayers

as the coating layer to cap the mesopore openings of the drug-loaded hollow mesoporous silica (HMS) particles.[21] However, many of the reported stimuli-responsive drug delivery systems have the gating features with poor biocompatibility, toxicity of the gating agents, or difficulty for using under physiological conditions.

In addition to the stimuli mentioned above, the use of enzymes is of great interest for triggering a responsive controlled drug release from a gated MSNs-based delivery system. Enzymes offer key advantages as release triggers, because they are not biologically disruptive, function under mild conditions, and possess a high degree of selectivity.[22-23] To date, several reports on the use of enzyme-mediated hydrolysis of supermolecules or polymeric components for the controlled opening of the gated MSNs carriers have been described.[24-29] For example, Bernardos et al. reported the synthesis of a lactose-capped MSNs for controlled release.[26] The $[Ru(bipy)_3]^{2+}$ dye could release from the lactose-capped MSNs after the addition of β-D-galactosidase to uncap the openings by the rupture of a glycosidic bond.[26]

It has been well known that nucleic acids are widely existed in the body, and have been recognized as attractive building blocks for nanobiotechnology and materials science owing to the remarkable specificity and versatility of these units.[30-32] Importantly, nucleic acids could be hydrolyzed by specific endonucleases. Therefore, it can be speculated that nucleic acids as a gating agent to cap the mesopore openings of MSNs carriers would achieve the enzyme-triggered controlled drug release, and this also could solve the problems of many reported gating agents

with poor biocompatibility, toxicity, or difficulty for using under physiological conditions.

Herein we designed and constructed an enzyme-triggered drug delivery system that is based on cytosine-phosphodiester-guanine oligodeoxynucleotide (CpG ODN)-capped hollow mesoporous silica (HMS) particles as carriers. As shown in Fig. 1, HMS particles were prepared by using a carbon sphere templating method reported in our previous work.[33-34] HMS particles were first loaded with a model drug, fluorescein dye, and then the external surfaces were grafted with (3-aminopropyl)triethoxysilane (APTES: $(C_2H_5O)_3SiCH_2CH_2CH_2NH_2$) to obtain the dye-loaded and aminated HMS particles (Dye/HMS-NH_2). Subsequently, the negatively charged CpG ODN interacted with the Dye/HMS-NH_2 particles due to the positively charged amino groups on the surface of the dye-loaded HMS particles, resulting in the capping of mesopore openings to obtain CpG ODN-capped HMS delivery system (Dye/HMS-NH_2/CpG). Finally, the uncapping of mesopore openings was triggered by the addition of deoxyribonuclease I (DNase I) for CpG ODN degradation, and allowing fluorescein molecules to release from the delivery system. Reports on such an enzyme-triggered drug delivery system have not been found before.

Experimental

Preparation of the dye-loaded and aminated HMS particles (Dye/HMS-NH_2): Firstly, HMS particles were prepared by a carbon sphere templating method according

to our previous report with some changes of synthesis parameters (see Supporting Information).[33-34] The Dye/HMS-NH_2 particles were prepared following the literature procedures after a little modification.[17] Typically, 500 mg of HMS particles and 34.4 mg of fluorescein dye were suspended in 50 ml of anhydrous ethanol inside a sealed bottle. Subsequently, the mixture was stirred during 24 h at 37 ^oC in dark with the aim of achieving maximum loading in the hollow cavities and mesopores of HMS particles. Afterward an excess of 3-aminopropyltriethoxysilane (1.5 ml, Aldrich) was added, and the suspension was continuously stirred for 24 h in dark. Finally, the yellow product (Dye/HMS-NH_2) was centrifuged, washed with ethanol, and dried at 70 ^oC for 12 h.

Preparation of CpG ODN-capped HMS delivery system (Dye/HMS-NH_2/CpG): Natural phosphodiester (PD) CpG ODN 2006 (sequence: 5'-TCGTCGTTTTGTCGTTTTGTCGTT-3') was diluted in the sterilized water to a concentration of 1 μg/μl and stored at -20 °C until use. Typically, at the weight ratio of 10 (Dye/HMS-NH_2 particles to CpG ODN, Dye/HMS-NH_2/CpG ODN), 20 μl of CpG ODN was added to 200 μl of the Dye/HMS-NH_2 suspension (1 μg/μl), and the resulting mixture was continuously shaken at 4 ^oC for 2 h, followed by centrifugation and washing with the sterilized water for five times to remove the residual free dye and CpG ODN.

Gel electrophoresis: For free CpG ODN and the Dye/HMS-NH_2/CpG particles, the samples at CpG ODN concentration of 5 μg/μl were prepared and stored at -20 ^oC. For HMS and the Dye/HMS-NH_2 particles, the concentration was same as that of the

Dye/HMS-NH_2/CpG suspension. Then, free CpG ODN, HMS, Dye/HMS-NH_2 and Dye/HMS-NH_2/CpG suspensions were used for gel electrophoresis experiment. Typically, 10 μl of the suspension was loaded into the gel, and electrophoresis was carried out at 180 V for 55 min running with a 1×TBE buffer according to the manufacturer's instructions. Ethidium bromide was used to visualize CpG ODN using a UV transilluminator (Dolphin-Doc, Kurabo industries Ltd.) at 312 nm.

To optimize the necessary amounts of CpG ODN for capping on the Dye/HMS-NH_2 particles, gel electrophoresis experiments were used to confirm the optimal weight ratio of Dye/HMS-NH_2/CpG ODN. The Dye/HMS-NH_2 particles were reacted with CpG ODN for 2 h at various weight ratios from 5 to 50 Dye/HMS-NH_2/CpG ODN. After centrifugation (15000 rpm, 10 min), the supernatant was recovered and loaded into the gel, and electrophoresis was carried out at 180 V for 55 min running with a 1×TBE buffer according to the manufacturer's instructions. Ethidium bromide was used to visualize CpG ODN using a UV transilluminator (Dolphin-Doc, Kurabo industries Ltd.) at 312 nm.

In vitro release behavior of the Dye/HMS-NH_2/CpG particles: *In vitro* release of fluorescein dye from the Dye/HMS-NH_2/CpG particles was carried out with a shaking bed at 37 ^{o}C. Typically, 200 μg of the Dye/HMS-NH_2/CpG particles was immersed into 1 ml of Tris buffer (20 mM Tris, 100 mM NaCl, 10 mM $MgCl_2$, 1mM $CaCl_2$, pH 7.4) in a 1.5 ml tube (DNase I concentration of 0, 1, 2.5 and 5 U/ml), and the tube was fixed on shaking bed with a 100 rpm of shaking speed. After a predetermined time interval, 5 μl of the suspension was removed and centrifuged, and the supernatant was

used for quantitative analysis of fluorescein dye at the wavelength of 494 nm on a NanoDrop 2000 spectrometer.

Characterization methods: Scanning electron microscopy (SEM) was carried out with a Hitachi S4800 field emission scanning electron microscope. Transmission electron microscopy (TEM) was performed with a JEM-2000FX electron microscope operated at an acceleration voltage of 200 kV. N_2 adsorption-desorption isotherms were obtained on a Quantachrome Autosorb 1C apparatus at -196 ^{o}C under continuous adsorption conditions. Zeta potential measurements were conducted on laser electrophoresis zeta-potential analyzer (LEZA-600, Otsuka, Japan). UV/Vis spectra were recorded on a NanoDrop 2000 spectrometer.

Results and discussion

The representative SEM and TEM images of HMS particles are shown in Fig. 2. Similar to our previous reported results,[33-34] these spherical particles are well monodisperse, and have hollow structure. The average particle size is in the range of 400-500 nm, and the silica shell is about 70-80 nm in thickness. From the high magnification TEM image in Fig. 2c, disordered mesopores are distributed on the shells.

Furthermore, it can also be observed that only one small particle is encapsulted in the hollow cavity of each HMS particle. Our previous report have demonstrated that the small particle is Fe_3O_4 particle.[33] Because the carbon sphere templates were adsorbed with iron precusor, Fe_2O_3 particle could be formed in the hollow cavity

during the calcination in air at 550 ^{o}C to remove the carbon sphere template. After the reduction in 5% H_2/95% Ar at 350 ^{o}C for 2h, the Fe_2O_3 particle was transformed to Fe_3O_4 particle. Therefore, these HMS particles exhibited a ferromagnetic property with the M_s (magnetization saturation) value of 1.25 emu/g (Fig. 2d), which might be potential for magnetic targeting delivery.

The N_2 adsorption–desorption isotherm of HMS particles can be classified as type IV isotherm, typical curve for mesoporous materials (Fig. 3). The specific surface area was 683.5 m^2/g calculated from the linear part of the BET (Brunauer-Emmett-Teller) plot, and the single point adsorption total volume at P/P_0 = 0.90 was 0.511 cm^3/g (Tab. 1). The corresponding pore size distribution curve calculated from the desorption branch by the BJH (Barrett-Joyner-Halenda) method showed a narrow pore size distribution peaked at 2.6 nm (inset of Fig. 3), allowing small fluorescein molecules to diffuse into the hollow cavities through the mesoporous shells.

Dye loading and amino-grafting on HMS particles were characterized by UV/Vis spectra, zeta potential and N_2 adsorption–desorption measurements. The UV/Vis spectrum of the Dye/HMS-NH_2 particles shows the characteristic UV/Vis absorption peak at 494 nm for fluorescein dye (Fig. 4), suggesting fluorescein dye has been loaded in HMS particles. As shown in Fig. 5, the zeta potential of HMS particles was -23.2 mV, while that of the Dye/HMS-NH_2 particles was 7.7 mV, which confirms the positively charged amino groups have been grafted on the surface of the dye-loaded HMS particles. Therefore, the Dye/HMS-NH_2 particles are able to interact with the

negatively charged CpG ODN, resulting in the capping of mesopore openings for the Dye/HMS-NH_2 particles. N_2 adsorption–desorption measurement further confirmed the fluorescein dye loading and amino-grafting on HMS particles (Fig. 3). After the fluorescein dye loading and amino-grafting on HMS particles, the significant decreases in the N_2 volume adsorbed, specific surface area (287.2 m^2/g), pore size (< 2 nm) and pore volume (0.196 cm^3/g) were observed, which indicates a decrease of the porosity, resulting from a high content of fluorescein dye filling the mesopores and amino-grafting on the surface of the dye-loaded HMS particles.

The formation of the Dye/HMS-NH_2/CpG particles was driven mainly by electrostatic interaction between the negatively charged CpG ODN and the positively charged Dye/HMS-NH_2 particles. As expected in Fig. 5, the capping of CpG ODN on the Dye/HMS-NH_2 particles caused a reversal in zeta potential from 7.7 mV to -16.3 mV, which qualitatively demonstrates a successful CpG ODN capping to the surface of the Dye/HMS-NH_2 particles.

In general, DNA migration on the agarose gel can be retarded after DNA bonding on the particles.[35] In this study, the CpG ODN capping to the Dye/HMS-NH_2 particles was also investigated by an agarose gel electrophoresis. As shown in Fig. 6, the HMS and Dye/HMS-NH_2 particles (lane 1 and 2) have not any band on the gel owning to no CpG ODN on the particles. While for the Dye/HMS-NH_2/CpG particles (lane 4), the CpG ODN was completely retained in the sample well with no electrophoresis shift corresponding to free CpG ODN (lane 3), which suggests that CpG ODN has been capped to the Dye/HMS-NH_2 particles by the interaction between

amino groups of the Dye/HMS-NH_2 particles and phosphate groups of CpG ODN.

Also, UV/Vis spectrum further confirmed the fluorescein dye loading and CpG ODN capping to the Dye/HMS-NH_2/CpG particles. As shown in Fig. 4, after CpG ODN capping to the Dye/HMS-NH_2 particles, the characteristic absorption peaks of fluorescein dye and CpG ODN at 494 and 260 nm, respectively, could be observed on the UV/Vis spectrum of the Dye/HMS-NH_2/CpG particles, suggesting that the Dye/HMS-NH_2/CpG particles have loaded with the fluorescein dye and been capped with CpG ODN. Compared to the the Dye/HMS-NH_2 particles, the Dye/HMS-NH_2/CpG particles exhibited a little decrease of the absorbance at 494 nm, which is attributed to the decrease of fluorescein amount in the Dye/HMS-NH_2/CpG particles due to the release during the CpG ODN capping on the the Dye/HMS-NH_2 particles and washing process.

To optimize the necessary amounts of CpG ODN for capping to the Dye/HMS-NH_2 particles, gel electrophoresis experiments were used to confirm the optimal weight ratio of Dye/HMS-NH_2/CpG ODN. As shown in Fig. 7, the CpG ODN band in the supernatant became weaker with an increase in the weight ratio and disappeared at a weight ratio of ≥ 20, suggesting that CpG ODN was able to cap to the Dye/HMS-NH_2 particles, and that all of CpG ODN molecules were capped to the Dye/HMS-NH_2 particles at a weight ratio of ≥ 20. In order to all grafted amino groups on the surfaces of the Dye/HMS-NH_2 particles could interact with CpG ODN to cap the mesopores, the weight ratio of ≤ 15 should be used to cap the mesopore openings of the Dye/HMS-NH_2 particles.

To determine the fluorescein dye loading capacity and CpG ODN capping amount on the Dye/HMS-NH_2/CpG particles, the Dye/HMS-NH_2/CpG particles with the weight ratio of 10 was investigated. The fluorescein dye amount in the Dye/HMS-NH_2 particles was 52.4 μg/mg by elemental analysis and thermogravimetric analysis. The final fluorescein dye loading capacity in the Dye/HMS-NH_2/CpG particles was 37.7 μg/mg, which was determined from the dye amount of the Dye/HMS-NH_2 particles after the interaction with CpG ODN by measuring the absorbance of the released fluorescein dye at 494 nm during the capping and washing processes. Compared to MCM-41,[17] HMS exhibited a higher fluorescein dye loading capacity using the similar loading method. Also, CpG ODN capping amount on the Dye/HMS-NH_2/CpG particles was 39.6 μg/mg, which was determined by measuring the absorbance of CpG ODN at 260 nm before and after the interaction with the Dye/HMS-NH_2 particles.

To investigate the enzyme-triggered controlled release of fluorescein dye from the Dye/HMS-NH_2/CpG particles, DNase I was used as a representative endonuclease for CpG ODN degradation. Fig. 8A shows the release behavior of fluorescein dye from the Dye/HMS-NH_2/CpG particles in the absence and in the presence of DNase I. The Dye/HMS-NH_2/CpG particles exhibited a negligible release of fluorescein dye in the absence of DNase I, thus indicating that CpG ODN was tightly capped to the mesopore openings. After the addition of DNase I with a 5 U/ml concentration, fluorescein dye was fast released from the Dye/HMS-NH_2/CpG particles owning to the uncapping of the mesopore openings, and exhibited a sustained release manner.

Furthermore, the release rate of fluorescein dye can be controlled by changing the concentration of DNase I solution. As shown in Fig. 8B, the release rate of fluorescein dye increased with the increase of the DNase I concentration. The release of fluorescein dye depends on the enzymatic degradation of CpG ODN cappings. The higher DNase I concentration led to the faster degradation rate of CpG ODN cappings, thus resulting in the increased release rate of fluorescein dye. Therefore, the CpG ODN-capped HMS particles could be promising for enzyme-triggered drug delivery.

Conclusion

We have successfully designed an enzyme-triggered drug delivery system that is based on CpG ODN-capped HMS particles as carriers and responds to DNase I stimuli. HMS particles provided high drug loading capacity, and amino-grafting on the surface of the dye-loaded HMS particles made the negatively charged CpG ODN to cap the mesopore openings by the interaction between the amino groups of the Dye/HMS-NH_2 particles and the phosphate groups of CpG ODN. Drug release was triggered by the addition of DNase I for CpG ODN degradation, and the drug release rate from the Dye/HMS-NH_2/CpG particles can also be controlled by changing the concentration of DNase I. Therefore, it might be promising to use nucleic acids as gating agent for preparation of biocompatible and enzyme-triggered drug delivery system based on HMS particles.

Acknowledgements

The authors gratefully acknowledge the support provided by the Opening Project of State Key Laboratory of High Performance Ceramics and Superfine Microstructure (No. SKL201004SIC) and the Starting Fund from University of Shanghai for Science and Technology (No. 10-00-310-001).

Reference:

[1] C. T. Kresge, M. E. Leonowicz, W. J. Roth, J. C. Vartuli, J. S. Beck, *Nature,* **1992**, *359*, 710-712.

[2] M. Vallet-Regí, F. Balas, D. Arcos, *Angew. Chem. Int. Ed*. **2007**, 46, 7548 -7558.

[3] A. J. Di Pasqua, K. K. Sharma, Y.-L. Shi, B. B. Toms, W. Ouellette, J. C. Dabrowiak, T. Asefa, *J. Inorg. Biochem.* **2008**, 102, 1416-1423.

[4] M. Vallet-Regí, A. Rámila, R. P. del Real, J. Pérez-Pariente, *Chem. Mater.* **2001**, 13, 308-311.

[5] Y. Zhu, J. Shi, W. Shen, H. Chen, X. Dong, M. Ruan, *Nanotechnology*, **2005**, 16, 2633-2638.

[6] Y. Zhu, J. Shi, *Micropor. Mesopor. Mater.* 2007, 103, 243-249.

[7] S. Wang, *Micropor. Mesopor. Mater*. **2009**, 117, 1-9.

[8] J. L. Vivero-Escoto, I. I. Slowing, B. G. Trewyn, V. S.-Y. Lin, *Small*, **2010**, 6, 1952-1967.

[9] M. Manzano, M. Vallet-Regí, *J. Mater. Chem*. **2010**, *20*, 5593–5604.

[10] L. L. Li, F. Q. Tang, H. Y. Liu, T. L. Liu, N. J. Hao, D. Chen, X. Teng, J. Q. He, *ACS Nano*, **2010**, 4, 6874-6882.

[11] Q. He, J. Shi, *J. Mater. Chem*. 2011, 21, 5845-5855.

[12] N. K. Mal, M. Fujiwara, Y. Tanaka. *Nature* **2003**, 421, 350-353.

[13] R. Liu, Y. Zhang, X. Zhao, A. Agarwal, L. J. Mueller, P. Feng, *J. Am. Chem. Soc*. **2010**, 132, 1500-1501.

[14] S. Giri, B. G. Trewyn, M. P. Stellmaker, V. S.-Y. Lin, *Angew. Chem. Int. Ed*. **2005,**

44, 5038-5044.

[15] C. Y. Lai, B. G. Trewyn, D. M. Jeftinija, K. Jeftinija, S. Xu, S. Jeftinija, V. S.-Y. Lin, *J. Am. Chem. Soc*. **2003**, 125, 4451-4459.

[16] Z. Luo, K. Cai, Y. Hu, L. Zhao, P. Liu, L. Duan, W. Yang, *Angew. Chem. Int. Ed*. **2011**, 50, 640-643.

[17] E. Climent, R. Martínez-Mánez, F. Sancenón, M. D. Marcos, J. Soto, A. Maquieira, P. Amorós, *Angew. Chem. Int. Ed*. **2010**, 49, 7281-7283.

[18] C. Chen, J. Geng, F. Pu, X. Yang, J. Ren, X. Qu, *Angew. Chem. Int. Ed*. **2011**, 50, 882-886.

[19] E. Climent, A. Bernardos, R. Martínez-Mánez, A. Maquieira, M. D. Marcos, N. Pastor-Navarro, R. Puchades, F. Sancenón, J. Soto, , P. Amorós, *J. Am. Chem. Soc*. **2009**, 131, 14075-14080.

[20] R. Casasús, E. Climent, M. D. Marcos, R. Martínez-Mánez, F. Sancenón, J. Soto, , P. Amorós, J. Cano, E. Ruiz, *J. Am. Chem. Soc*. **2008**, 130, 1903-1917.

[21] Y. Zhu, J. Shi, W. Shen, X. Dong, J. Feng, M. Ruan, Y. Li, *Angew. Chem. Int. Ed.* **2005**, 44, 5083-5087.

[22] P. D. Thornton, R. J. Mart, S. J. Webb, R. V. Ulijn, *Soft Matter*. **2008**, 4, 821-827.

[23] Y. Itoh, M. Matsusaki, T. Kida, M. Akashi, *Biomacromolecules*, **2006**, 7, 2715-2718.

[24] K. Patel, S. Angelos, W. R. Dichtel, A. Coskun, Y.-W. Yang, J. I. Zink, J. F. Stoddart, *J. Am. Chem. Soc*. **2008**, 130, 2382-2383.

[25] C. Park, H. Kim, S. Kim, C. Kim, *J. Am. Chem. Soc*. **2009**, 131, 16614-16615.

[26] A. Bernardos, E. Aznar, M. D. Marcos, R. Martínez-Mánez, F. Sancenón, J. Soto, J. M. barat, P. Amorós, *Angew. Chem. Int. Ed*. **2009**, 48, 5884-5887.

[27] A. Schlossbauer, J. Kecht, T. Bein, *Angew. Chem. Int. Ed*. **2009**, 48, 3092-3095.

[28] P. D. Thornton, A. Heise, *J. Am. Chem. Soc*. **2010**, 132, 2024-2028.

[29] A. Bernardos, L. Mondragon, E. Aznar, M. D. Marcos, R. Martínez-Mánez, F. Sancenón, J. Soto, J. M. Barat, E. Perez-Paya, C. Guillem, P. Amorós, *ACS Nano*, **2010**, 4, 6353-6368.

[30] P. Alberti, J. Mergny, *Proc. Natl. Acad. Sci. USA*, **2003**, 100, 1569-1573.

[31] Y. W. Kwon, C. H. Lee, D. H. Choi, J. I. Jin, *J. Mater. Chem*. **2009**, 19, 1353-1380.

[32] C. M. Niemeyer, *Angew. Chem. Int. Ed*. **2001**, 40, 4128-4158.

[33] Y. Zhu, E. Kockrick, T. Ikoma, N. Hanagata, S. Kaskel, *Chem. Mater.* **2009**, 21, 2547-2553.

[34] Y. Zhu, T. Ikoma, N. Hanagata, S. Kaskel, *Small* **2010**, 6, 471-478.

[35] I. Y. Park, I. Y. Kim, M. K. Yoo, Y. J. Choi, M.-H. Cho, C. S. Cho, *Inter. J. Pharm.* **2008**, 359, 280–287.

Tab. 1 The structure parameters of the HMS and Dye/HMS-NH_2 particles

samples	S_{BET} (m^2/g)	V_p (cm^3/g)	D_p (nm)
HMS	683.5	0.511	2.6
Dye/HMS-NH_2	287.2	0.196	< 2

Figure Captions:

Fig. 1 Scheme of preparation of the Dye/HMS-NH_2/CpG particles and enzyme-triggered drug release.

Fig. 2 (A) SEM, (B, C) TEM images of HMS particles and (D) the magnetization curve measured at 300 K for HMS particles.

Fig. 3 The N_2 adsorption-desorption isotherms of the HMS and Dye/HMS-NH_2 particles and corresponding pore size distributions (insert).

Fig. 4 UV/Vis spectra of the samples before and after the fluorescein dye loading and CpG ODN capping.

Fig. 5 The zeta potential of the HMS, Dye/HMS-NH_2 and Dye/HMS-NH_2/CpG particles.

Fig. 6 Gel electrophoresis of the HMS (lane 1), Dye/HMS-NH_2 (lane 2) suspensions, free CpG ODN solution (lane 3) and the Dye/HMS-NH_2/CpG suspension (lane 4).

Fig. 7 Gel electrophoresis of the supernatants after the interaction between CpG ODN and the Dye/HMS-NH_2 particles at various weight ratios using agarose gel in TBE running buffer.

Fig. 8 (A) Enzyme-triggered release switching of fluorescein dye from the Dye/HMS-NH_2/CpG particles and (B) the release profiles of fluorescein dye from the Dye/HMS-NH_2/CpG particles at different concentrations of DNase I.

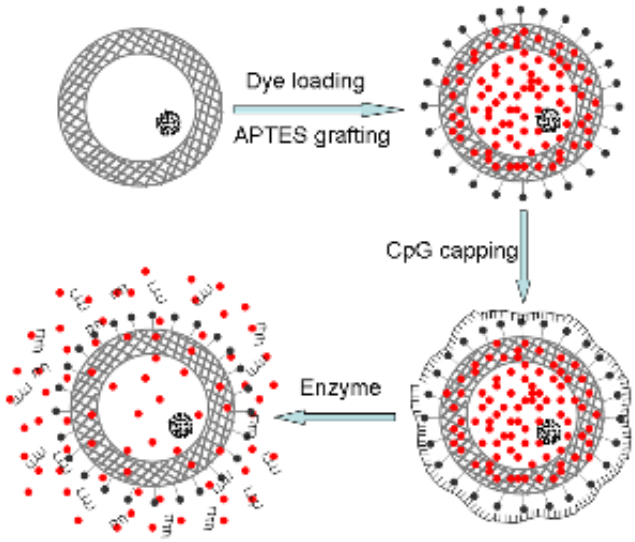

Fig. 1 Scheme of preparation of the Dye/HMS-NH_2/CpG particles and enzyme-triggered drug release

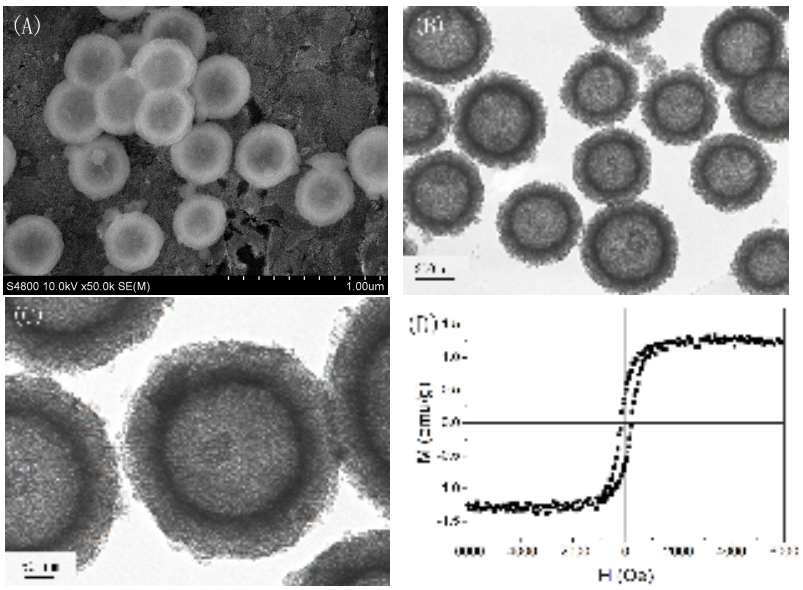

Fig. 2 (A) SEM, (B, C) TEM images of HMS particles and (D) the magnetization curve measured at 300 K for HMS particles

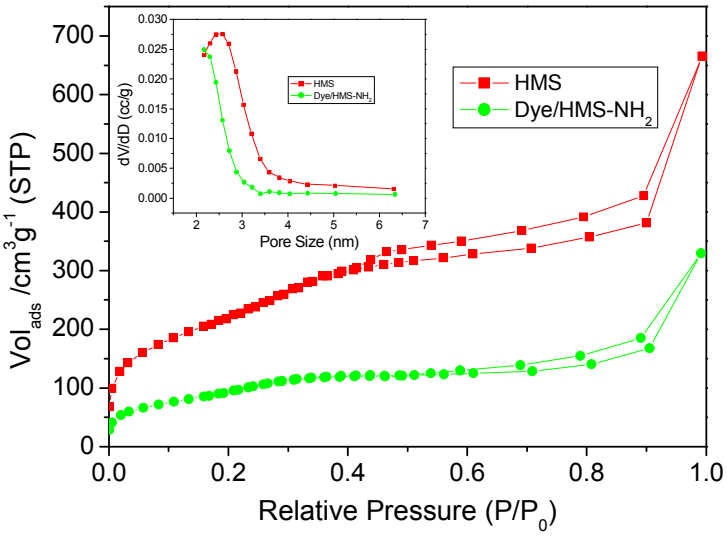

Fig. 3 The N_2 adsorption-desorption isotherms of the HMS and Dye/HMS-NH_2 particles and corresponding pore size distributions (insert)

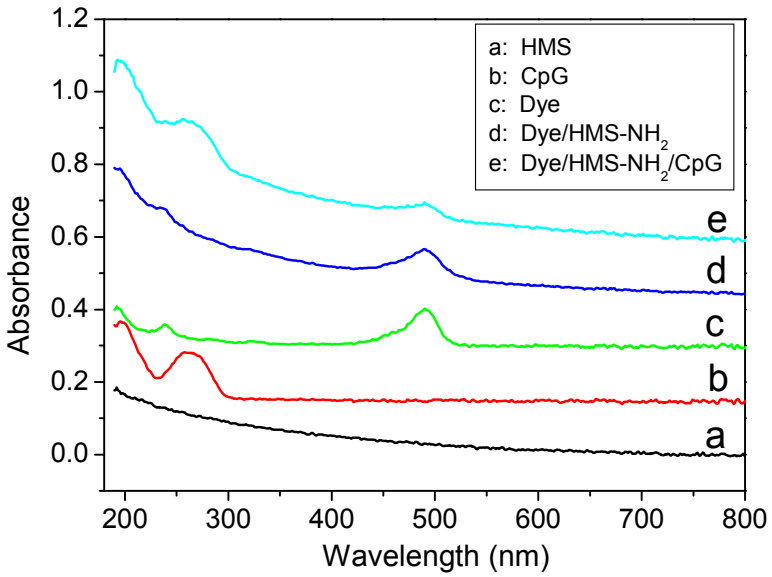

Fig. 4 UV/Vis spectra of the samples before and after the fluorescein dye loading and CpG ODN capping

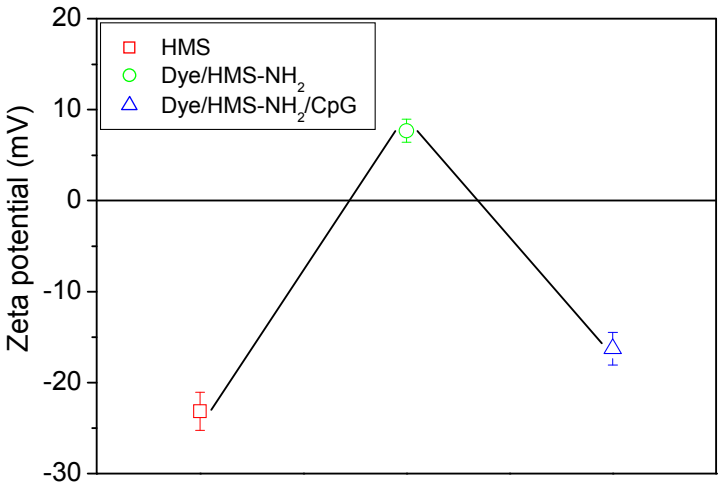

Fig. 5 The zeta potential of the HMS, Dye/HMS-NH_2 and Dye/HMS-NH_2/CpG particles

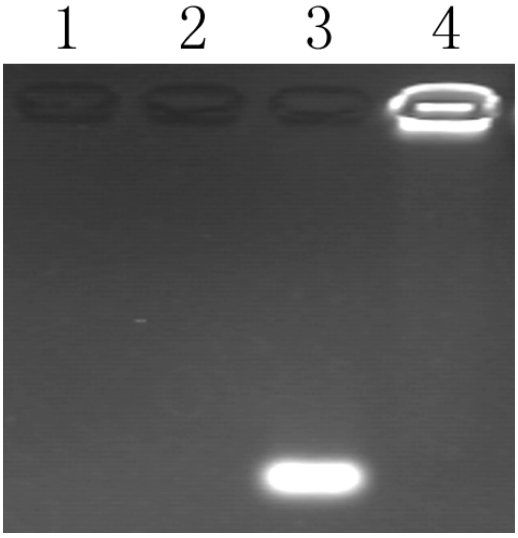

Fig. 6 Gel electrophoresis of the HMS (lane 1), Dye/HMS-NH_2 (lane 2) suspensions, free CpG ODN solution (lane 3) and the Dye/HMS-NH_2/CpG suspension (lane 4)

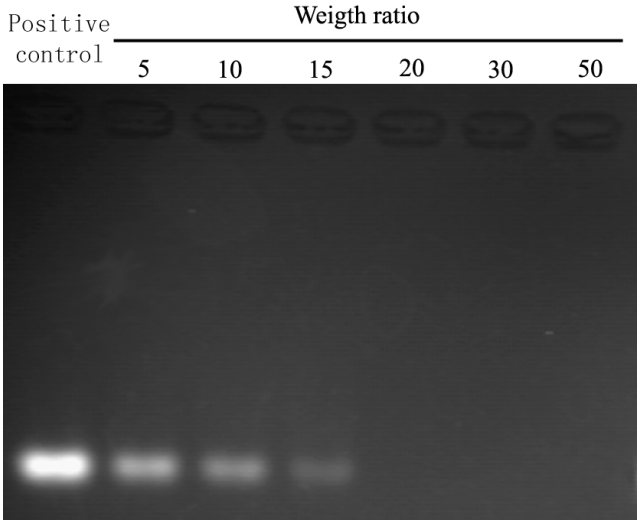

Fig. 7 Gel electrophoresis of the supernatants after the interaction between CpG ODN and the Dye/HMS-NH_2 particles at various weight ratios using agarose gel in TBE running buffer

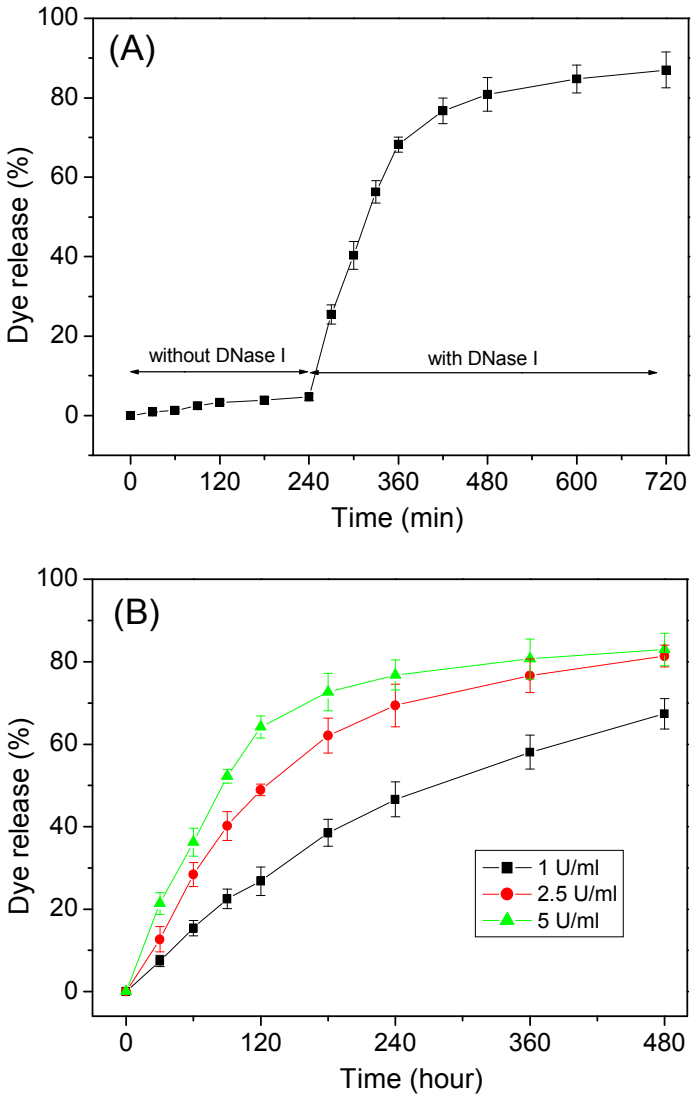

Fig. 8 (A) Enzyme-triggered release switching of fluorescein dye from the Dye/HMS-NH_2/CpG particles and (B) the release profiles of fluorescein dye from the Dye/HMS-NH_2/CpG particles at different concentrations of DNase I